Feedforward-Feedback Controller Using General Regression Neural Network (GRNN) for Laboratory HVAC System: Part I—Pressure Control

Osman Ahmed, Ph.D., P.E.
Member ASHRAE

John W. Mitchell, Ph.D., P.E.
Fellow ASHRAE

Sanford A. Klein, Ph.D.
Fellow ASHRAE

ABSTRACT

Variable-air-volume (VAV) systems are growing in popularity in the laboratory industry due to their ability to conserve energy. However, VAV systems pose new control challenges to achieve a stable and accurate performance over a wide range of operating conditions. A combined feedforward and feedback control approach is proposed in this paper with the objective to enhance performance, to be cost effective, and to be easy to implement and operate for laboratory HVAC systems. The feedforward component employs a general regression neural network (GRNN) for HVAC system identification and control, while the feedback component provides a control signal to offset any steady-state error.

This is Part I of a three-part paper that compares the performance of the combined control approach with conventional feedback and feedforward only controllers. The comparison is made for the control sequences commonly found in a laboratory with a VAV system. A general overview of the different control approaches is presented in this paper. The control sequence for pressure is developed, and a simulation model is built. Simulated results are then presented for the combined, feedforward only, and conventional feedback control approaches. The results clearly indicate that the combined approach performs better than the feedback approach over widely varying operating conditions and different damper characteristics. The combined approach is stable and eliminates all steady-state error.

INTRODUCTION TO LABORATORY HVAC SYSTEMS

The use of hazardous materials in a laboratory environment makes safety a major concern in its design and operation. A laboratory requires different control strategies than an office space to accommodate health and safety factors. Both the construction and operating costs of research buildings containing laboratories are high, reflecting the specialized nature of the building in terms of functions, service utilities, safety, security, and a host of other features.

Reliability, redundancy, flexibility, and monitoring requirements for lab HVAC systems differ from those for commercial space. Moreover, the lab safety and comfort requirements put additional constraints on the HVAC systems. The central HVAC system in a laboratory building treats outside air and then distributes it to different labs through ductwork. Typically, 100% outside air is drawn in by the air handler, conditioned, and then introduced to the lab space. On the exhaust side, a central fan exhausts air from the fume hoods and labs and discharges it to the atmosphere at a specified discharge velocity. In addition, effluents are exhausted through fume hood exhaust and by leakage from the laboratory. Fume hoods are controlled to maintain a constant average face velocity of air entering from the room. Although the fume hood exhaust system usually operates as a stand-alone system independent of the central HVAC system, it largely dictates the operation of the rest of the lab HVAC system.

The uniqueness of laboratory environments is well documented (ASHRAE 1995; Neuman 1989). The laboratory operating condition often changes rapidly due to the fume hood exhaust flows and laboratory equipment loads. The resulting dynamic pressure changes are often large. The lab HVAC system maintains a lower pressure in the lab space than in the adjacent spaces to induce infiltration into the lab space and prevent leakage of any contaminants. A properly maintained pressure differential is critical for both lab safety (Anderson 1987) and fume hood containment (Knutson 1987; Schuyler 1990; Ahmed and Bradley 1990). The value of pressure differential varies with the application and in the range of

0.005 in. to 0.05 in. of water (w.c.) (1.245 Pa to 12.45 Pa) (Wenz 1989; Neuman and Rousseau 1986; Esmond 1989; Baylie and Schultz 1994).

A constant-air-volume lab system, in parallel to the constant-air-volume fume hood operation, draws in and exhausts a constant volume of outdoor air based on the maximum design condition. The yearly energy cost of conditioning commercial space is about $2.00 to $3.00 per square foot (DOE/EIA 1991; DOE/HUD 1990). In contrast, the energy cost for a laboratory is in the range of $6.00 to $10.00 per square foot (Nelson 1986; Neuman and Rousseau 1986). A typical laboratory building is six to ten times more energy intensive than an office building of the same size (Moyer 1983). Energy costs can be reduced, however, if the supply air volume is varied, depending upon the activity in the lab space, similar to the variable-air-volume (VAV) fume hood operation. The total VAV approach saves energy and also increases VAV hood containment efficiency (Neuman and Rousseau 1986; Davis and Benjamin 1987; Neuman and Guven 1988). It has the ability to maintain space temperature, humidity, and pressure within close tolerance in critical applications and to produce stable and accurate performance over a wide range of operating conditions. The control of a VAV lab and HVAC system is explored in this paper.

LABORATORY CONTROL SYSTEMS

Figure 1 shows an overall control system for a VAV laboratory. Besides the stand-alone fume hood control, there are three distinct control loops working together to maintain the lab space comfortable and safe. The supply flow control loop is dependent upon the fume hood and general exhaust control systems and, to ensure safety, lags by always keeping the lab space pressure lower than in the adjacent spaces. The general exhaust control loop is used usually to provide cooling. The reheat coil/valve control loop provides heating in the space. The pressure control sequence is discussed in detail later in this paper, while the temperature control for heating and cooling sequences is described in companion papers, parts two and three (Ahmed et al. 1998a; Ahmed et al. 1998b), respectively.
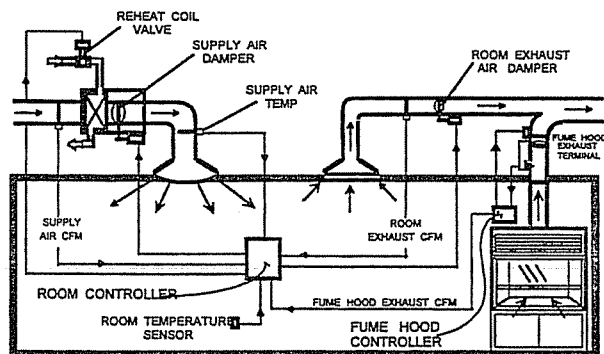

Figure 1   *A typical variable-air-volume laboratory HVAC control system.*

The fume hood controller controls the fume hood loop, while the room controller is responsible for controlling the flow rates of supply air, general exhaust, and reheat coil input. Both these controllers are local area network devices reporting to the building automation system. Figure 1 also shows the different sensors that measure system state variables (Hrkman 1996). Each individual local airflow control loop has a flow measuring device. The room temperature sensor measures room temperature. In addition, duct air discharge air temperature is also measured and used in the reheat coil/valve control loop. Finally, the pressure differential (DP) across the control dampers is also included.

The essence of the conventional lab control system is a feedback loop that uses a proportional-integral-derivative (PID) algorithm to compute the controller output signal based on the error between the measured process variable and the set point. The coil discharge air temperature, general exhaust flow, and supply flow loops work locally to maintain their own individual set points. The supply flow rate set point is determined in the room controller by adding the general exhaust flow and the fume hood exhaust flow set points. The general exhaust flow rate and coil discharge air temperature set points are calculated based on the error between the room temperature set point and the actual value.

Each of the subsystems described in Figure 1 has time-varying and nonlinear characteristics and operates over a wide range with coupling between the loops (Chen and Lee 1990; Borresen 1981). Like most chemical processes, there are recycle loops (Stoecker 1971) that make the dynamic process complex. For a lab space, the dynamics of the HVAC process include the room thermal characteristics; the air and water distribution pipes and ducts; HVAC system components such as valves, dampers, and coils; and control components such as actuators, sensors, digital/pneumatic interface, and controllers. Each subsystem and system component has different response times that make the indoor climate control complicated (Athienitis et al. 1990).

The need to respond rapidly to sudden changes in the lab operating conditions challenges the control system. The changes occur as a result of fume hood operation or internal loads. The internal load can change from 2 W/ft^2 to 70 W/ft^2 (21.52 W/m^2 to 753.50 W/m^2) within seconds (Neuman 1989). The response time of the HVAC zone controllers, therefore, has to be similarly fast to maintain room temperature. In contrast, the steady heat load in a commercial space varies within 5 W/ft^2 to 10 W/ft^2 (53.82 W/m^2 to 107.65 W/m^2) (ASHRAE 1995). The air change per hour rate (ACH) in a lab may vary from a minimum value of 6 ACH to 10 ACH to a maximum of 60 ACH or more (ASHRAE 1995; Davis and Benjamin 1987). As a result, room airflow requirements vary widely in a laboratory environment within a very short period. Further, in many applications the temperature needs to be maintained within close tolerance. The task of a good lab controller, therefore, is to provide accurate and stable control

over a wide range of operations with a response time in the range of seconds.

Current methods of feedback controllers using proportional-integral (PI) or PID loops have inherent problems dealing with higher order nonlinear systems, a wide range of operation, variable system gains, and multiple interacting loops that are the characteristic of a lab environment. Tuning of PI/PID loops is a major commissioning issue, and current tuning processes are valid for single loops and often require trial and error to tune multiple, interconnected loops.

CONTROL APPROACHES

In the following sections, feedback control, the proposed strategy of combined feedforward and feedback control, and feedforward only control are discussed. The benefits and limitations of the combined approach are discussed in detail. The implementation scheme of the combined approach for laboratory pressure control is developed. A brief discussion of the general regression neural network (GRNN) used as an identifier and a controller in the feedforward block is included. A simulation model is developed that includes the tuning of control loops and combining feedforward and feedback control blocks. The results obtained by simulating three distinct control loops for pressure control sequence are compared.

The feedback controller uses the error between the set point and the measured variable as an input. The most common approach of employing feedback is the traditional linear PID algorithm. In a PID controller, the tuning parameters are derived for a specific operating range. Feedback control is simple to implement and performs well as long as the operating range and the set points do not vary significantly. Moreover, the linear PID controller does not perform well for nonlinear systems, and derivative control adds unneeded complexity and tuning difficulty in most HVAC applications (Haines and Hittle 1983). A well-tuned PI can achieve the desired response. The PI algorithm is selected as the basis of comparison against the combined algorithm.

A combined feedforward and feedback control topology is proposed as an alternative to the current feedback control method. The goal is to provide superior set-point tracking with the feedforward element, while the feedback element will provide steady-state disturbance rejection capability.

There is a considerable amount of published literature on the applications of a combined approach. Psaltis et al. (1987) proposed such a combined controller using a back-propagation neural network algorithm in the feedforward block. Kraft and Campagna (1990) found that a similar control topology performed better in the presence of noise for both linear and nonlinear systems when compared with a self-tuning regulator and a model reference adaptive controller. The authors commented that the combined approach is most favorable from the implementation point of view due to its simple algorithm. Combined feedforward and feedback controllers have been successfully used in the NASA Deep Space Network

antennas project (Gawronski and Mellstrom 1994). A combined feedforward and feedback approach has been successfully implemented for the control of semiconductor wafer temperature (Norman and Boyd 1992).

It is expected that a combined feedforward and feedback approach for a laboratory HVAC system may be appropriate. The feedforward controller can respond quickly and exhibit superior set-point tracking ability while the feedback controller rejects any steady-state disturbance. For lab applications, the command tracking will reduce the swing in control variables (i.e., temperature) and increase the comfort level. Since it bypasses the feedback loop, the controller response time also decreases. Moreover, if the feedforward path works well, the tuning of the feedback loop is simplified as it can then be designed to handle the disturbance rejection based on a small consistent error between the set point and the state variable. Simplified tuning and elimination of retuning will offer major cost advantages to the lab owners both in terms of commissioning and operation.

IDENTIFICATION OF EQUIPMENT CHARACTERISTICS

The feedforward controller will perform best if it can invert the control equipment characteristics such that for a given value of manipulated variable, the required signal to achieve that value is produced. For example, a damper/actuator assembly produces an output of airflow for a control signal input by modulating the damper position. If the input-output relationship of the damper is inverted, then the controller will be able to generate the required control signal for the desired airflow rate. Since the characteristics of the control equipment vary over time, some means of adaptation is necessary for recognizing such change.

The objective of this research is to find a solution that can be implemented in real controllers. With that objective in mind, a memory-based neural network is selected here that captures the input-output regression (linear or nonlinear) characteristics of the system. The neural network requires only a single parameter, and unlike back propagation, it does not involve any iterative training process. This GRNN has a theoretical basis using the Parzen window estimator (Parzen 1962) and was first applied as a neural network by Specht (1991). The GRNN is chosen as the algorithm to replicate the coil and valve characteristics due to its simplicity, robustness, and excellent capability in system identification. Unlike a conventional neural network, it requires minimal computational time to effectively capture the system characteristics. Specht (1991) discusses the theory of GRNN in detail. The following is a brief description of GRNN that illustrates its implementation in identification of the HVAC components.

The input to a GRNN is a series of data that can have multiple dimensions. For sample values of X_i and Y_i of input vector X and the scalar output Y, an estimate for the desired value of $\hat{Y}$ at any given value of X is found using all of the sample values in the following relations:

$$\hat{Y}(X) = \frac{\sum_{i=1}^{n} Y_i \exp\left(-\frac{D_i^2}{2\sigma^2}\right)}{\sum_{i=1}^{n} \exp\left(-\frac{D_i^2}{2\sigma^2}\right)} \qquad (1)$$

where the scalar function D_i^2, representing the Euclidean distance from the given value, is given by

$$D_i^2 = (X - X_i)^2 (X - X_i) \qquad (2)$$

and is the single smoothing parameter of the GRNN.

Equations 1 and 2 are the essence of the GRNN method. The estimate $\hat{Y}(X)$ is a weighted average of all the observed samples, Y_i, where each sample is weighted exponentially according to its Euclidean distance from each X_i denoted by D_i.

A GRNN algorithm represented in neural network architecture is shown in Figure 2. For a given X, the connections
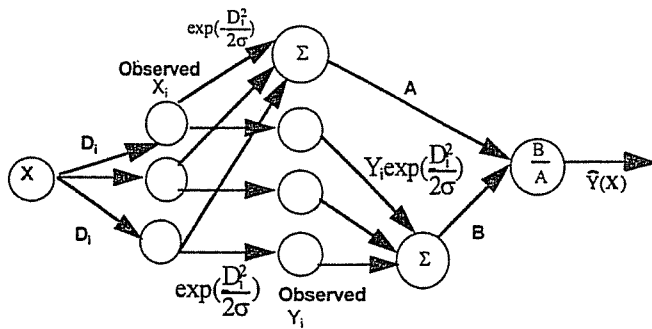

Figure 2 *General regression neural network architecture.*

between the input and the first layers compute the scalar D_i, based on observed samples X_i and smoothing parameter σ, and then takes the exponent of D_i^2. A node in the second layer sums up the exponential values for all samples. The other nodes calculate the product of the exponent value and the corresponding observed output Y_i for each sample observation. The node in the third layer adds up all the product values; this is then supplied to the output node where the ratio between the sum of the exponent and the product values is calculated. Compared to the back propagation method, the weighting coefficients between the layers are dependent only upon the observed samples of X_i, Y_i, and smoothing parameter σ. As a result, instead of training the weighting coefficients, only a suitable single value of σ is needed to predict the output. The optimum value of σ can be calculated by a simple yet effective scheme known as the "Holdout" method (Specht 1991).

The implementation of the GRNN to the characteristics of a heating coil or valve/damper also offers advantages over the conventional methods of identification. In a traditional regression method for identification, the operator has to input a priori knowledge of the equation type or has to search for the best fit

equation exhaustively. The code requirement for a nonlinear regression is intensive and may be prohibitive for online use in a controller. In contrast, the GRNN does not require any user input for the functional form of the characteristics and uses a strikingly simple code. Moreover, the GRNN algorithm can be imbedded into a hardware processor, thereby eliminating software development process to a large extent since software coding during field installation is not necessary. The choice of sample size and specific sample values are important in designing a GRNN in general. However, such issues are not so critical for HVAC applications. Only a small data set that covers the normal operating range of HVAC equipment is necessary.

One of the key components in the HVAC system is the airflow damper. The installed authority dictates the ultimate performance of the damper in a system. For example, an inherently linear damper will exhibit nonlinear performance as the authority becomes smaller. The authority is defined as the ratio of pressure loss across the damper to the total system pressure when the valve is fully open.
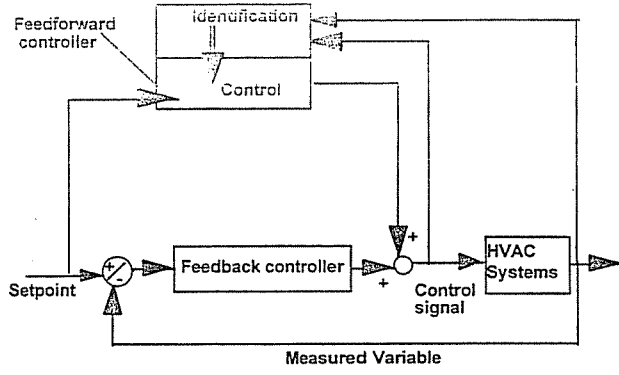
Expressing the damper characteristics in terms of authority, percent valve open, and percent maximum flow rate is typical (ASHRAE 1992). The damper authority can be calculated in real time by measuring the pressure differential across the damper and the total system pressure loss, or it can be estimated using a calibrated duct flow/pressure loss relationship and flow set point for each damper. The supply flow set point is also known based on steady-state mass balance, as explained later in this chapter.

The inverse of the physical process is used to generate the characteristics needed for a controller to produce the required control signal, C_s, for a desired flow set point, $\dot{v}_{a|sp}$, and given damper authority, a. The GRNN essentially captures and updates such characteristics from observed data (i.e., Figure 2) relating C_s to the supply flow rate and damper authority. Hence, for a given $\dot{v}_{a|sp}$ and a, the feedforward block will be able to generate the desired control signal of C_s. The feedback controller will then be able to compensate for small residual error with the identification process.

It is proposed that the GRNN will be used as an individual control equipment identifier. A large data set is not required for static mapping of HVAC equipment, i.e., valve/damper characteristics; hence, the GRNN will be a viable option. Besides, the GRNN does not require training, and a single smoothing factor can be initially determined based on the size of the input data set. Therefore, a combined feedforward and feedback controller will be proposed using the GRNN as system identifier for the lab HVAC system. Such an architecture is presented in detail in the following section.

TOPOLOGY FOR PRESSURE CONTROL

Figure 3 illustrates a general scheme of a combined feedforward and feedback loop along with its implementation for a supply flow control system. The GRNN is used as the identification block. Ahmed et al. (1997, 1996a) discussed the

A general feedforward-feedback scheme

Implementation of combined controller for supply flow roop

Figure 3 *Combined feedforward-feedback controller.*

applications of a combined approach for HVAC systems in great detail.

The feedforward only approach does not include the feedback block. The identification block still captures and updates the process characteristics based on the process input control signals and the measured variables and passes the updated characteristics periodically to the control block for control action. In this context, feedforward control does have a feedback mechanism to compensate for the system change. The main difference between feedback and feedforward control is that in feedback control, the control output is entirely dependent on the error, while in a feedforward controller, the feedback mechanism only influences the identification process.

The proposed combination feedforward and feedback, referred to as FFPI hereinafter, is compared with the feedback control method. For the sake of simplicity, a PI controller is chosen as a feedback method instead of PID. In addition, open loop control, hereinafter referred to as FF control, is also included for comparative analysis.
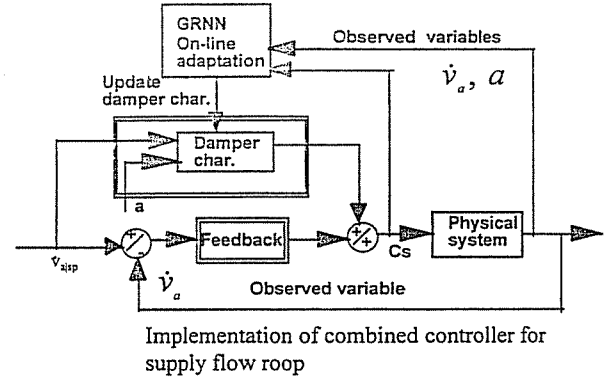
The PID controller is represented as a simple PI controller specifically suited for HVAC applications (Bekker et al. 1991). The PI controller is selected because it was developed for HVAC processes that are commonly found in coils and valve/damper actuators, which are often modeled as first-order linear systems with delay. Such models are also assumed to represent coil and actuator dynamics as a part of the lab simulator. The tuning of the PI control is based on the root-locus method (Bekker et al. 1991). A simple digital version for the control signal $C_{s,m}$ from a PI can be stated as follows (Mollenkamp 1981):

$$C_{s,m} = C_{s,m-1} + P_g(e_m - e_{m-1}) + I_g S_t e_m \qquad (3)$$

where the gains I_g and P_g are tuned according to the following equations:

$$I_g = \frac{1}{d_t S_g} e^{-1} \qquad (4)$$

and

$$P_g = \frac{\tau}{d_t S_g} e^{-1} \qquad (5)$$

For a given first-order system, the system gain, S_g, the delay time, d_t, and the time constant, τ, can be found easily from the open loop response of the process. The pneumatic actuators that are used for lab environments usually respond within a couple of seconds from closed to fully open position (Landis & Gyr 1994). In order to achieve such response time, the dead time and time constant are adjusted and the resultant response curve is shown in the top plot of Figure 4. Such a response curve is used to tune the PI controller (Mollenkamp
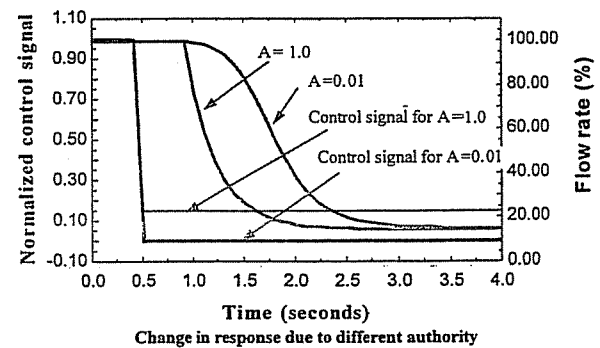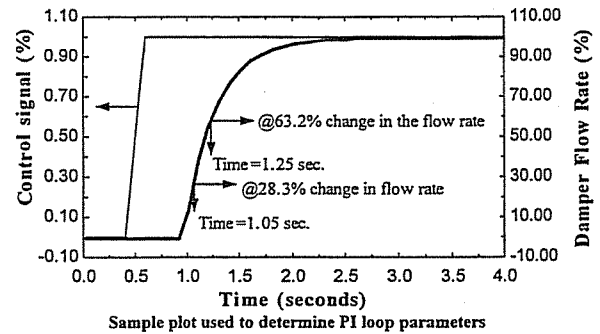

Sample plot used to determine PI loop parameters

Change in response due to different authority

Figure 4 *Open loop response of a linear damper/actuator.*

5

1981). The bottom plot of Figure 4 shows the open loop response of a linear damper for two different authorities. The impact of slow response for authority = 0.01 is explained later in the results section (case P3).

The system gain is defined as the ratio between the change in the output variable to the input variable. In Figure 4, the change in the input variable (i.e., control signal) is changed from 0% to 100%, resulting in a change of 100%. The corresponding change in the output variable (i.e., flow rate) is the same for a linear damper. Hence, the system gain, S_g, is 1.0. The time constant, τ, is the time the output variable takes to reach 63.20% of the final value less the delay time. Hence, by definition and by noting the time to reach 63% change, from Figure 3, the sum of delay and time constant is

$$\tau + d_t = 1.25 \text{ seconds}. \tag{6}$$

Similarly, another expression for one-third of time constant can be written as the amount of time the output variable takes to achieve 28.3% of the total change excluding the delay time. Noting this time to be 1.05 seconds, the relation is

$$\frac{1}{3}\tau + d_t = 1.05 \text{ seconds}. \tag{7}$$

Solving equations 6 and 7 yields $\tau = 0.3$ second and $d_t = 0.95$ second. Inserting these values along with S_g into Equations 4 and 5, the controller gains are obtained: $P_g = 0.116$ and $I_g = 0.387$. Further fine tuning, by trial and error, was necessary to make the loop respond without undershoot or overshoot and to achieve good response performance comparable to the response obtained from the FFPI controller. The final values of the tuning parameters are $P_g = 0.188$ and $I_g = 0.617$.

The room pressure is typically controlled in terms of a differential instead of an absolute value. The differential is the difference between a reference space (i.e., an adjacent corridor) and the lab space. The goal in a lab is to keep the differential pressure positive within a range of 0.005 w.c. to 0.05 w.c. This ensures that the room pressure remains lower than the adjacent pressure under all operating conditions to prevent the leakage of lab air to adjacent spaces.

SIMULATION MODEL

A simple control sequence is modeled to assess the performance of different control methods for pressure control. A change in the fume hood exhaust requires modulation of the supply airflow to maintain the differential pressure set point. The thermal effect is decoupled from the pressure effect by assuming that the temperatures of supply, exhaust, and infiltration air are constant at 70°F (21.11°C). In a typical pressure control sequence, the fume hood exhaust jumps from a steady-state condition to a maximum value as the hood sash is opened. As a result, the lab pressure decreases, which makes the differential pressure go higher. The control senses the deviation between the actual differential pressure and the set point and opens the supply flow to return the set point.

The control methods were compared using a laboratory simulator that consists of a room, reheating coil, valve and damper, actuator, sensors, and controller. The development of this simulator is discussed in several earlier publications (Ahmed et al. 1996a, 1996b, 1997; Ahmed 1993, 1996) and not repeated here due to space constraints. The simulator's controller block was modified as needed to replicate various control methods.

The simulation was carried out using Engineering Equation Solver (EES) software (Klein and Alvarado 1998). The EES uses a variant of Newton's method to solve nonlinear algebraic equations, while a variant of the trapezoid rule with a second-order predictor-corrector algorithm is used for solving differential equations.

The simulation sample time is chosen to be 0.1 seconds. The simulation sample time is adequate compared to the time constant of 0.3 seconds, as two to three samples in a time constant are usually used for a digital controller (Dorf 1980). The simulation sample time of 0.1 second means about 17 to 18 samples during end-to-end damper stroke, which is also adequate according to the published literature (Haines and Hittle 1983; Weaver 1983).

The feedforward components uses the steady-state mass balance and infiltration equations to solve for the supply flow set point. The steady-state mass balance for laboratory space is

$$\dot{m}_s + \dot{m}_{ad} - \dot{m}_e = 0 \tag{8}$$

Using the ideal gas law and expressing mass flow rate in terms of pressure, temperature, and volume flow rate, the above equation can be written as

$$\frac{P_{s,sp}\dot{v}_{s,sp}}{T_{s,sp}} + \frac{P_{ad,sp}\dot{v}_{ad,sp}}{T_{ad,sp}} - \frac{P_{sp}\dot{v}_{e,sp}}{T_{sp}} = 0 \tag{9}$$

The infiltration relation is

$$\dot{v}_{ad,sp} = K_1(\Delta P_{sp})^n \tag{10}$$

The laboratory pressure differential, ΔP_{sp}, is defined as a differential:

$$\Delta P_{sp} = P_{ref,sp} - P_{sp} \tag{11}$$

In the above equations, the laboratory supply airflow rate set point, $\dot{v}_{s,sp}$; total laboratory exhaust set point, $\dot{v}_{e,sp}$; and supply air discharge temperature set point, $T_{s,sp}$, are unknowns with other parameters known from the design data. The total laboratory exhaust is a sum of general exhaust and exhaust from fume hoods and is given by

$$\dot{v}_{e,sp} = \dot{v}_{fh,sp} + \dot{v}_{ex,sp} \tag{12}$$

In a VAV laboratory, the fume hood exhaust set point is a known quantity for each position of the fume hood sash. Hence, by determining the set point for total laboratory exhaust, the general exhaust set point will be known. For the

pressure control sequence, $\dot{v}_{ex, sp}$ is zero since the general exhaust damper is only opened during cooling sequence, as explained in Part III of this paper. The method of calculating laboratory supply airflow rate set point, $\dot{v}_{s, sp}$, depends on the selection of pressure control strategy.

There are two common methods of laboratory space pressure control. In the flow tracking approach, the supply flow set point is determined by assuming a fixed difference between the laboratory exhaust and supply flow set point. In the direct approach, a differential pressure sensor is usually mounted near the entrance door. The error between the differential pressure set point and the actual value is calculated first and then fed into a PID algorithm that produces an output of supply flow set point. The two severe limitations of the direct approach are exceptional sensitivity to very small values of pressure differential (i.e., 0.0025 kPa) and the fact that the measured pressure differential becomes zero when the door is opened (Hitchings 1994). The flow tracking method is more prevalent in the industry.

Once the supply flow rate set point, $\dot{v}_{s|sp}$, is known, then a conventional PI loop can be utilized to achieve the flow set point. This is a significant shift from the traditional approach in which the flow set point is determined by assuming a fixed difference between the lab exhaust and supply flow set point. Hence, by knowing the total lab exhaust set point, the supply flow set point can easily be calculated. The traditional method is known as volume tracking and has serious limitations because, often, the difference in flow is simply assumed based on experience (Ahmed 1993; Ahmed et al. 1993). The limitations include over- or underpressurization of the lab space if the difference in flow is selected incorrectly. The FFPI and PI control strategy models, as used in the simulations, are shown in Figure 5.

In the case of FFPI control, for a known supply flow rate set point, the identified damper characteristics are used to generate the required control signal. The combined FFPI approach uses a PI control loop in conjunction with the loop to eliminate the steady-state error. The PI control loop only
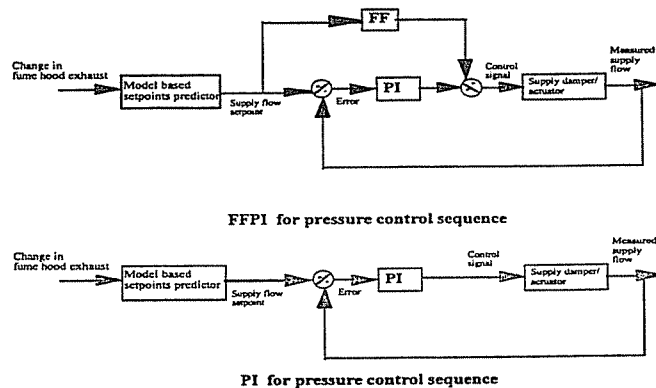

FFPI for pressure control sequence

PI for pressure control sequence

Figure 5 *Schematics of combined and feedback controllers.*

works with the error between the set point and the simulated flows.

Several options were considered in order to combine the outputs from the feedforward and feedback controllers. The detailed analysis is found in the published reference (Ahmed 1996) and is described only briefly here. A simple switch is used to set the control signal from the PID algorithm to zero whenever a set-point change is noticed, and then only the feedforward block produces a control signal when the set point is changed. The PID output is only added when the set point does not change, which indicates that the system is at steady state. This combination approach is based on the fact that feedback is only responsible for the steady-state error that will not be detected by the open feedforward block. It is reasonable to expect a relatively small steady-state error due to the uncertainties introduced with the identification scheme, measurement, and controller.

RESULTS

Control systems are judged on accuracy, robustness, stability, and ease of implementation. The ease of implementation is important for keeping the commissioning cost down and is often a major factor for an owner in selecting a specific control method for a given application. A lab control system should be capable of keeping the lab environment under tight control under a wide range of operations. Failure to do so translates into significant cost to the owner because the lab needs to be shut down and requires maintenance. This is especially true in a research or process lab where inadequate environmental conditions may cause a loss in productivity.

The three control methods were simulated and compared for six different damper characteristics and operating points. Three cases were for a linear damper with different authorities. Typically, a linear damper is installed, but it hardly stays as linear since the authority changes with varying system flows. The other cases are based on nonlinear damper characteristics and under different operating conditions. In the damper model (Kelly et al. 1984) used in the simulator, the term W_f represents the linearity. A value of 1.0 for W_f indicates a linear damper, whereas 0.0 means a true exponential damper. A W_f of 0.5 was chosen for nonlinear damper, while the authority varied between 0.1 and 0.01. The five damper characteristics are shown in Figure 6.

In laboratory pressure control, the change in fume hood flows is considered to be the disturbance function. Two different disturbance sequences were considered for the simulations. First, the total lab fume hood exhaust flow was reduced from a maximum of 2400 cfm to 500 cfm (1133 L/s to 236 L/s) and then increased to 2400 cfm (236 L/s) again. The corresponding supply flow rates to maintain a space temperature of 70°F (21.11°C) and Δp of 0.05 w.c (12.45 Pa) are 2257 cfm (1065.3 L/s) and 357 cfm (172.3 L/s).

After comparing results for this sequence and noting that at the maximum flow, the operating point is more or less the same for different damper characteristics, another operating
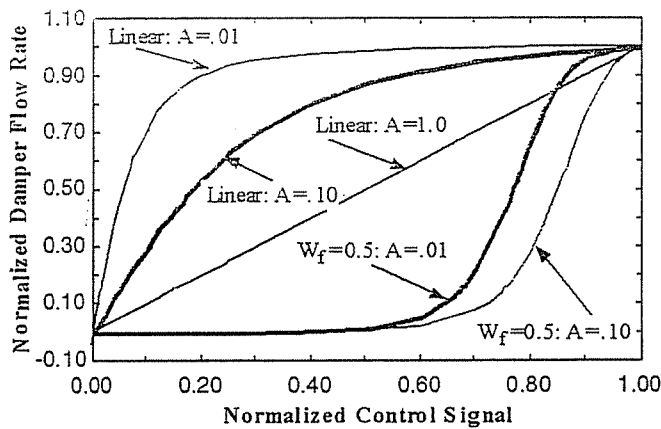
Figure 6 *Damper/valve characteristics for simulation.*

Figure 7 *Dynamic pressure response for control sequence P1.*

point was selected as the midpoint between the minimum and maximum flows, i.e., 1450 cfm (684.4 L/s). The results are discussed for each simulation case.

Case P1: Linear Damper with an Authority of 1.0

All of the different control loops are assumed to be tuned for this case. This assumption is appropriate since HVAC control equipment manufacturers usually calibrate and supply the valves, dampers, and actuators as linear, and during the commissioning process they are usually tuned at fully open positions and tuned one at a time. As a result, the pressure drop across the control equipment is a maximum and the authority achieves a value close to unity. The combined approach, FFPI, is also tuned for this case. The P and I gain are relatively very small for the FFPI loop compared to the PI loop. Table 1 lists tuning parameters for different control loops for various sequences.

All of the control loops for case P1 perform exceedingly well. The responses of the room differential pressure, Δp, are shown in Figure 7. The responses seem reasonable for the given disturbance in fume hood exhaust flow. As the fume exhaust flow suddenly decreases at the start of the sequence, the differential pressure ($\Delta_p = P_{ad} - P$) momentarily becomes negative, which means that the room remains at a higher pressure than the adjacent room until the supply flow reduces to match the exhaust flow for the correct differential. The reverse takes place when the fume hood exhaust is increased from a minimum flow. The PI has zero offset under steady state, and the under- and overshoots are very comparable to those for FF and FFPI approaches.
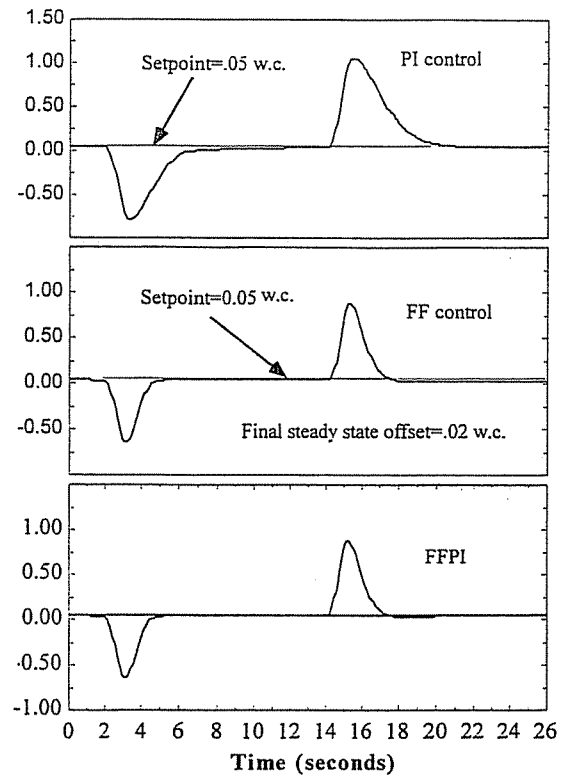
In the case of open loop control (FF), considerable offsets are noted for both sequences when the room pressure becomes positive as a result of a sudden decrease in the fume hood exhaust flow and vice versa. However, using the combined loop, FFPI, the offsets are eliminated while the response time and the under- and overshoots remain the same.

Case P2: Linear Damper with an Authority of 0.1

For the case C2, the authority is changed from 1.0 to 0.1, while other simulation parameters remain the same. Figure 8 shows that the performance of PI controller remains unchanged with respect to the response time when compared to case 1 except that the undershoot has increased. At the maximum flow condition, both the stability and the set point are achieved. The open loop response remains similar to that with an authority of 1.0 and shows both over- and undershoots. The response of the FFPI loop is good with zero offset and a quick response.

TABLE 1
Table of Controller Gains

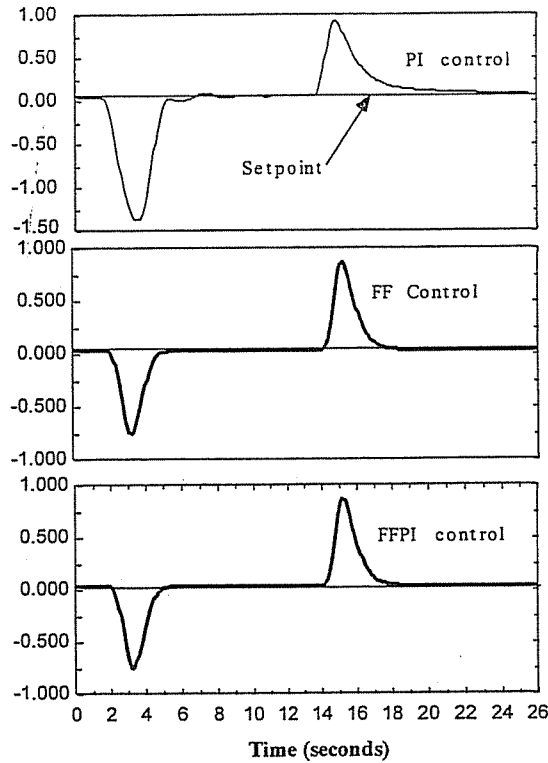| Control Sequence	Control Equipment	FFPI Controller		PI Controller	
		P_g (Control Signal/Error)	$I_g S_t$ (Control Signal/Error)	P_g (Control Signal/Error)	$I_g S_t$ (Control Signal/Error)
Pressure	Supply damper	5.0 e(-6)	2.5 e(-5)	0.188	.061

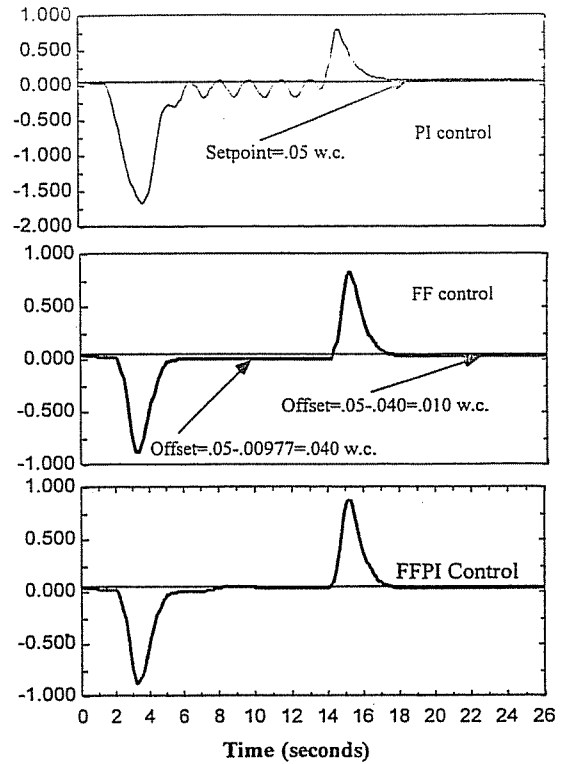**Figure 8** Dynamic pressure response for control sequence P2.

Figure 9 Dynamic pressure response for control sequence P3.

Case P3: Linear Damper With an Authority of 0.01

The responses of different control loops are shown in Figure 9. The results show that the PI controller in this case becomes unstable at the low end of the flow for $a = 0.1$. For the feedback loop, the controller seems to do much better when the flow is increased. As expected, the FF loop reacts rapidly but has offsets. The combined loop, FFPI, eliminates such offsets and responds very quickly. With the decrease in the flow set point from 2400 cfm (1132.8 L/s) to 500 cfm (236 L/s), the Δp undershoots to almost –1.00 w.c. (–249 Pa) for both FF and FFPI loops, compared to –0.75 w.c. (186.75 Pa) in the case of $a = 1.0$ (Case P1 in Figure 7). The significant undershoot can be explained in that the damper is modeled as a linear first-order differential equation with time constant τ_{act} and dead time t_o as shown below.

$$\tau_{act}\frac{dr_{ac}}{dt} + r_{ac} = r_{sp,\,(t-t_o)} \tag{13}$$

The solution for the above differential equation can be expressed as

$$r_{ac} = br_{ac,\,(t-t_o)} + (1-b)r_{sp,\,(t-t_o)} \tag{14}$$

where

$$b = e^{-\left(\frac{S_t}{\tau_{act}}\right)} \tag{15}$$

The command signal, r_{ac}, to the actuator in equation 14 is obtained by adding two terms. The first term is a product of a constant exponential term, b, and the command signal sample taken t_o time before the current sample time. The second term is a product of a constant exponential term, $1-b$, and the command signal set point taken t_o time before the current sample time. Equation 14 clearly shows that for a given value of b, the actuator response will be slow if the difference between the actuator set point and the current command signal is large and vice versa. As the flow set point reduces from 2257 cfm to 357 cfm (1065.3 L/s to 168.5 L/s) (i.e., 98% to 15% of maximum flow of 2303 cfm [1087 L/s]), the required control signal set point to produce 15% flow was found to be about 0.016 for $a = 0.01$ whereas the value is 0.15 for $a = 1.0$ (Figure 6). The difference between the current actuator command signal, r_{ac}, and the set point, r_{sp}, is larger for an authority of 0.01 than for the authority of $a = 1.0$. The flow response, therefore, is slow for a damper having $a = 0.01$ when the flow set point is decreased. Due to the slow response, it takes a longer time for the damper/actuator to reach the low flow position. As a result, the lab becomes positively pressurized, causing a larger undershoot in Δp. The response is shown in Figure 4.

In the last three cases, P4, P5, and P6, a nonlinear damper is considered instead of a linear damper. As a part of the damper model, the damper nonlinearity parameter, W_f, of 1.0 represents a linear damper, whereas a value of 0.0 indicates a true exponential damper. It is possible for a linear damper to exhibit the nonlinear characteristics due to mechanical problems. For simulation purposes, a W_f of 0.5 is chosen.

Figure 10 shows the response curves for various control loops. The PI, in this case, shows stable control as the exhaust flow is decreased from 2400 cfm to 500 cfm (1132.8 L/s to 236 L/s). In this case, the combined approach works well in providing good stability and eliminating the steady-state offset observed for the FF control loop.

Case P5: Nonlinear Damper, W_f = 0.5, a = 0.10, Flow Increased to 1450 cfm

A test was performed to evaluate the performance when the flow was increased to a mid-range value of 1450 cfm (684.40 L/s) instead the full range of 2400 cfm (1132.8 L/s). The objective here is to observe the controller performance for an operating point that lies on the nonlinear portion of the damper curve for a = 0.1 (Figure 5) and that deviates considerably from the corresponding point on a linear characteristic. For example, a flow of 1450 cfm (684.40 L/s) is about 60% of the maximum flow. Hence, for a linear damper/actuator, a

control signal of 60% is required to achieve 1450 cfm (684.40 L/s). However, referring Figure 6, a control signal of about 22% is required to generate 1450 cfm (684.40 L/s) for a damper with an authority of 0.10.

The results in Figure 11 show that the PI controller still performed well when the exhaust flow was decreased. In fact, the undershoot in Δp was considerably less compared to Case P2 under the same condition of decrease in the exhaust flow rate. As the exhaust flow increased in the mid-range, severe instability was observed with the PI loop as expected because the damper was operating within the nonlinear portion of the damper curve (Figure 6). The PI remains unstable throughout the entire sequence. The combination FFPI controller shows good trends.

Case P6: Nonlinear Damper, W_f = 0.5, a = 0.01, Flow Increased to 1450 cfm

The last case is considered by assuming an authority of 0.01 for a nonlinear damper. The resultant highly nonlinear damper characteristic is shown in Figure 6. The PI loop shows stability when the exhaust flow is decreased, while instability is noted when the exhaust flow is increased from the minimum to the mid-range. The FFPI achieved the same results as before providing stability, fast response, accuracy, and zero offset error under steady state. The pressure responses for different control loops are shown in Figure 12.
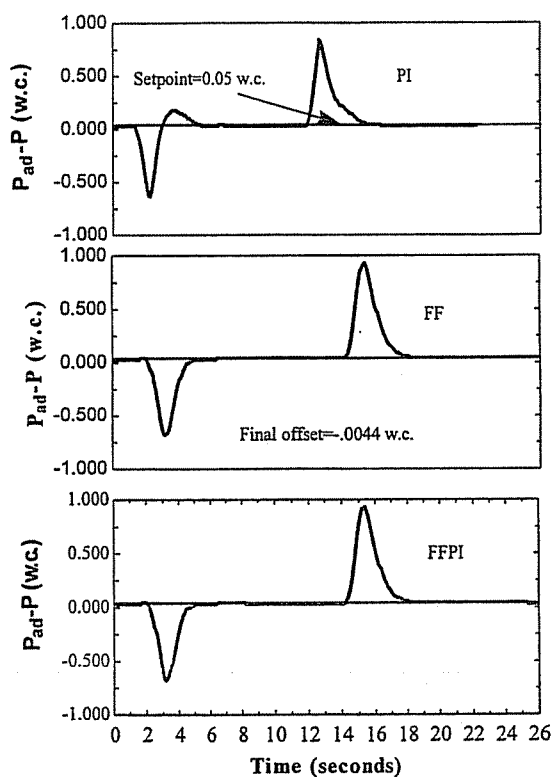

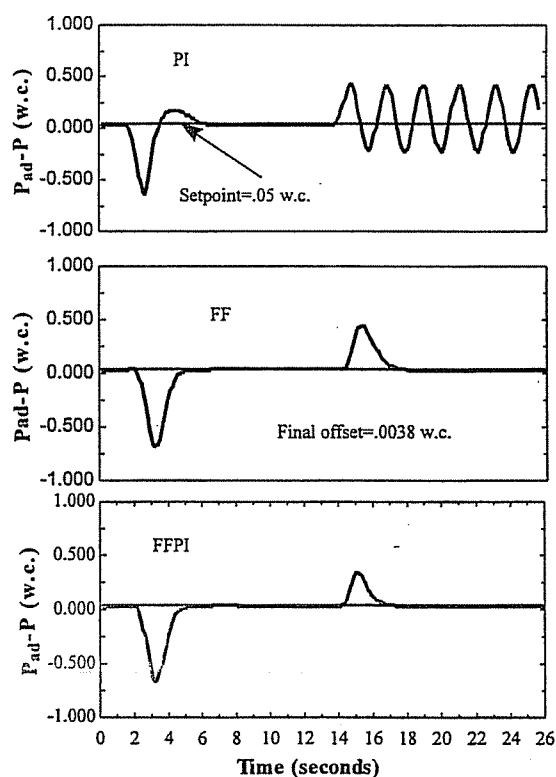Figure 10 *Dynamic pressure response for control sequence P4.*

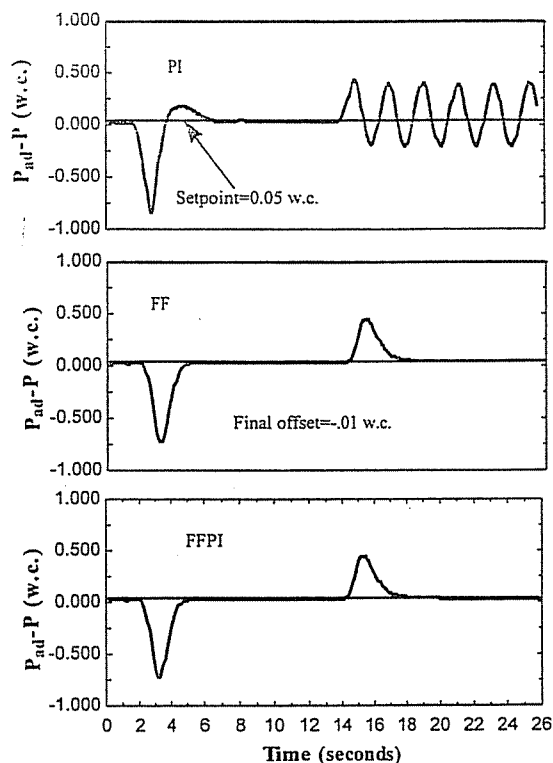Figure 11 *Dynamic pressure response for control sequence P5.*

Figure 12 *Dynamic pressure response for control sequence P6.*

CONCLUSIONS

The cases for pressure control sequences are selected with an objective of evaluating controller performance under wide operating conditions and with different damper characteristics. The combined feedforward/feedback controller performs well for each case and produces stable and accurate control. The PI controller performs well only at the peak operating condition and at the tuned condition. A feedforward only controller also worked well in providing quick and stable control for different cases, although there is an offset. For noncritical applications, where tight pressure control is not required, a feedforward only control may be adequate provided it can adapt to changing damper characteristics.

A model-based approach is used in order to determine the supply flow set point. It is expected that the model-based approach will overcome limitations of current approaches that determine the set point by subtracting a constant offset from total laboratory exhaust volume flow rate. Volume tracking may over- or underpressurize the lab space if the value of constant offset between the laboratory exhaust and supply flow rates is chosen incorrectly. The model-based approach eliminates this problem.

The combined approach of control is further explored for laboratory temperature control sequences in Part II and Part III of this paper. At the end of Part III, a more elaborate conclusion and recommendations section is included based on the observed results discussed in all three parts.

NOMENCLATURE

a	=	damper/valve installed authority
ACH	=	room air change per hour rate
C_s	=	control signal
D_g	=	derivative gain constant in PID controller
d_t	=	delay time
e	=	error between set point and observed value
FF	=	feedforward
FFPI	=	combined feedforward and feedback
I_g	=	integral gain constant in PID controller
K_l	=	envelope leakage constant
$\dot{m}$	=	rate of mass flow, lbm/sec (kg/s)
n	=	flow exponent
P	=	pressure, inches of water, kPa
Δp	=	pressure differential, in. of water, kPa
PI	=	proportional-integral
PID	=	proportional-integral-derivative
P_g	=	proportional gain constant in PID controller
S_t	=	sample time, seconds
t_o	=	dead time, seconds
T	=	temperature, °F (°C)
V	=	volume, ft^3 (m^3)
$\dot{v}$	=	volumetric flow rate, ft^3/min (m^3/min)
W_f	=	nonlinear valve/damper parameter
w.c.	=	inches of water column gauge
w.g.	=	inches of water column gauge
X	=	random GRNN input vector
X	=	given sample of GRNN input vector
X_i	=	ith observed sample of GRNN input vector X
Y	=	random GRNN output scalar
Y	=	desired GRNN output for given input vector X
$\hat{Y}$	=	estimate of desired GRNN output Y
Y_i	=	ith observed sample of GRNN output scalar Y

Greek Symbols

τ	=	time constant, seconds

Subscripts

ad	=	adjacent space
e	=	exhaust
ex	=	general exhaust
fh	=	fume hood
s	=	supply
sp	=	set point

REFERENCES

Ahmed, O. 1993. A design method for laboratory pressurization. CLIMA 2000 conference, London, U.K.

Ahmed, O., J.W. Mitchell, and S.A. Klein. 1998a. Feed-forward-feedback controller using general regression neural network (GRNN) for laboratory HVAC system: Part II—Temperature control—Cooling. *ASHRAE Transactions* 104(2).

Ahmed, O., J.W. Mitchell, and S.A. Klein. 1998b. Feed-forward-feedback controller using general regression neural network (GRNN) for laboratory HVAC system: Part III—Temperature control—Heating. *ASHRAE Transactions* 104(2).

Ahmed, O., J.W. Mitchell., and S.A. Klein. 1997. Feedforward-feedback HVAC controller using general regression neural network. IFAC Symposium on Artificial Intelligence in Real Time Control, Kuala Lumpur, Malaysia.

Ahmed, O., J.W. Mitchell, and S.A. Klein. 1996a. Application of general regression neural network (GRNN) in HVAC process identification and control. *ASHRAE Transactions* 102(1).

Ahmed, O., J.W. Mitchell, and S.A. Klein. 1996b. Influence of heat load on selection of laboratory design parameters and dynamic performance of laboratory environment. *ASHRAE Transactions* 102(1).

Ahmed, O., and S.A. Bradley. 1990. An approach to determining the required response time for a VAV fume hood control system. *ASHRAE Transactions* 96(2).

Ahmed, O., J.W. Mitchell., and S.A. Klein. 1993. Dynamics of laboratory pressurization. *ASHRAE Transactions* 99(2).

ASHRAE. 1992. *ASHRAE handbook—Systems and equipment*, Chapter 20. Atlanta: American Society of Heating, Refrigerating and Air-Conditioning Engineers, Inc.

ASHRAE. 1995. *ASHRAE handbook—HVAC applications*, Chapter 13, Laboratories. Atlanta: American Society of Heating, Refrigerating and Air-Conditioning Engineers, Inc.

Anderson, S.A. 1987. Control techniques for zoned pressurization. *ASHRAE Transactions* 93(2).

Athienitis, A.K., M. Stylianou, and J. Shou. 1990. A methodology for building thermal dynamics studies and control applications. *ASHRAE Transactions* 96(2).

Baylie, C.L., and S.H. Schultz. 1994. Manage change: Planning for the validation of HVAC systems for a clinical trials production facility. *ASHRAE Transactions* 100(1).

Bekker, J.E., P.H. Meckl, and D.C. Hittle. 1991. A tuning method for first-order processes with PI controllers. *ASHRAE Transactions* 97(2).

Borresen, B.A. 1981. HVAC control process simulation. *ASHRAE Transactions* 87(2).

Chen, Y.H., and K.M. Lee. 1990. Adaptive robust control scheme applied to a single-zone HVAC system. *ASHRAE Transactions* 96(2).

Davis, S.J., and R. Benjamin. 1987. VAV with fume hood exhaust systems. *Heating/Piping/Air Conditioning*, August.

DOE/EIA. 1991. *Commercial building characteristics*. Publication DOE/EIA-0246(89), U.S. Government Printing Office, Washington D.C. Department of Energy/Energy Information Agency.

DOE/HUD. 1990. *Building energy performance standards*. Washington D.C.-U.S. Department of Energy and U.S. Department of Housing and Urban Development.

Dorf, R.C. 1980. *Modern control systems*. Reading, Mass.: Addison-Wesley Publishing Company.

Esmond, J. 1989. Research laboratory ventilation system. *Heating/Piping/Air Conditioning Magazine*, February.

Gawronski, W.K., and J.A. Mellstrom. 1994. Antenna servo design for tracking low-earth-orbit satellites. *Journal of Guidance, Control, and Dynamics*.

Haines, R.W., and D.C. Hittle. 1983. *Control systems for heating, ventilating, and air-conditioning*. New York: Van Nostrand Reinhold.

Hitchings, D.T. 1994. Laboratory space pressurization control systems. *ASHRAE Journal* February.

Hrkman, L. 1996. Lab controls lunch and learn presentation. Landis & Gyr, Buffalo Grove, Ill., February.

Kelly, G., C. Park, D.R. Clark, and W.B. May. 1984. HVACNSSIM+, A dynamic building-HVAC-control systems simulation program. Workshop on HVAC controls, modeling, and simulation, Atlanta: Georgia Institute of Technology.

Knutson, G.W. 1987. Testing containment of laboratory hoods: A field study. *ASHRAE Transactions* 93(2).

Klein, S.A, and F.L. Alvarado. 1998. Engineering equation solver. F-Chart Software, Middleton, WI.

Kraft, L.G., and D.P. Campagna. 1990. A comparison between CMAC neural network control and two traditional adaptive control systems. *IEEE Control Systems Magazine*.

Landis & Gir. 1994. *Laboratory control and safety solutions design guide*. Buffalo Grove, Ill: Landis & Gir Powers.

Mollenkamp, R.A. 1981. Modern digital and automatic process control. McGraw-Hill Chemical Engineering Seminar, McGraw-Hill, New York.

Moyer, R.C. 1983. Fume hood diversity for reduced energy consumption. *ASHRAE Journal*, September.

Norman, S.A., and S.P. Boyd. 1992. Multivariable feedback control of semiconductor wafer temperature. American Control Conference.

Nelson, J.S. 1986. Key design considerations for mechanical and electrical building and environmental systems. Paper presented at the 1986 Tradeline Conference on the R & D Facility of the Future, San Francisco, Calif.

Neuman, V.A. 1989. Design considerations for laboratory HVAC systems dynamics. *ASHRAE Transactions* 95(1).

Neuman, V.A., and H.M. Guven. 1988. Laboratory building HVAC systems optimization. *ASHRAE Transactions* 94(2).

Neuman, V.A., and W.H. Rousseau. 1986. VAV for laboratory hoods—Design and costs. *ASHRAE Transactions* 92(1A).

Parzen, E. 1962. On estimation of a probability density function and mode. *Annal of Mathematical Statistics*.

Psaltis, D., A. Sideris., and A.A. Yamamura. 1987. A multi-layered neural network controller. Paper presented at the

1987 IEEE International Conference on Neural Networks, San Diego, Calif.

Schuyler, G. 1990. Performance of fume hoods in simulated laboratory conditions. *ASHRAE Transactions* 96(2): 428-434.

Specht, D.F. 1991. A general regression neural network. *IEEE Transactions on Neural Networks.*

Stoecker, W.F. 1971. A generalized program for steady-state system simulation. *ASHRAE Transactions* 77(1).

Weaver, H.J. 1983. *Applications of discrete and continuous Fourier analysis.* New York: John Wiley & Sons.

Wenz, R.G. 1989. A practical laboratory ventilation control system. *ASHRAE Transactions* 95(2): 830-836.